

Experimental and Numerical Study of Heat Transfer and Tensile Strength of Engineered Porous Fins to Estimate the Best Porosity

Ali Heydari^{a*}, Mehrdad Mesgarpour^b, Mohammad Reza Gharib^a

^a Department of Mechanical Engineering, University of Torbat Heydarieh, Torbat Heydarieh, Khorasan Razavi, Iran

^b Fluid Mechanics, Thermal Engineering and Multiphase Flow Research Lab. (FUTURE), Department of Mechanical Engineering, King Mongkut's University of Technology Thonburi, Bangmod, Bangkok 10140, Thailand

Received May 22 2020

Accepted September 20 2020

Abstract

In porous media, increasing porosity improves heat transfer rate and pressure drop across the fluid flow while decreasing strength of the body. Therefore, determining the optimum porosity is a serious challenge in balancing these two functional components of porous environments. In this research, an experimental study and numerical modeling of heat transfer and mechanical strength of engineered porous fin have been performed. In this regard, the model to create the porous medium is selected as a network of connected spheres. In order to estimate the best porosity, the effect of the porosity variation in the allowed range is investigated to achieve the best heat transfer and tensile strength simultaneously for three different materials of copper, aluminum and brass. The results show that the tensile strength and heat transfer optimized simultaneously for a specific porosity for each material.

© 2020 Jordan Journal of Mechanical and Industrial Engineering. All rights reserved

Keywords: Fins; heat transfer; porous media; tensile strength; porosity;

1. Introduction

Heat transfer has always attracted the attention of engineers and researchers from various perspectives. Several studies have been conducted in the field of extended surfaces as the first candidate for increasing heat transfer. Porous medium can be considered as an excellent solution for heat transfer augmentation due to the high surface area. By changing the structure and engineering the porous medium, engineered porous medium (EPM) has been presented. In this concept, instead of random distribution of porosity and irregularity in the shape of cavities, we encounter a completely united structure with an accurate porosity designation and a regular shape of cavities in each of the three directions. However, in a typical porous medium constructed by casting, spray forming or gas injection processes, all physical properties, such as porosity are distributed arbitrarily.

In the pre-engineered process of porous body, after designing the medium, which is based on the requirements, it is possible to manufacture a piece by manufacturing technologies according to the pre-plan. In fact, the basic difference between a typical porous medium and an engineered porous medium is the pre-design process and precise arrangement that would lead to the highest possible effectiveness. In engineering applications, effectiveness and manufacturing prospects should be considered simultaneously. In addition, the life of the manufactured

part, with respect to cost, is an important factor. So, the enhancement in thermal efficiency should not be along with the reduction in strength and the life of the piece. In general, metal foams are widely used as a porous medium to increase heat transfer. The advantage of using foams or fins that are designed as a network of connected spheres is that their porosity can be purposefully changed into different functions. For example, where conduction is essential, the spheres should be more compact, and the foam has less porosity. Where convection heat transfer is important, less spherical compaction and more porosity should be considered. On the other hand, the strength of these engineered fins must be considered. These fins can be a good alternative to solid (uniform) fins or heat sinks in the industry as less material is needed for construction while having higher heat transfer rates.

Numerous numerical, experimental and analytical investigations have been carried out on the topic of heat transfer in porous media such as [1-3]. Among the studies for developing the theoretical topics, the work of Hatami et al. [4] can be mentioned. They proposed a numerical solution method for solving the heat transfer equations in the porous fins which showed that the perturbation and repeating variable methods are the effective for solving nonlinear equations of convection and radiation.

Bejan and Morega [5] investigated the effect of thermal resistance on the porous fin. They revealed that the fins' arrangement and porosity percentage have a great influence on the flow regime, and consequently, the temperature

* Corresponding author e-mail: a.Heydari@torbath.ac.ir

distribution of the porous fins. Jeng and Tzeng performed a numerical analysis of heat transfer in the porous fins [6]. They showed that in the lower Reynolds numbers, the highest Nusselt number occurs at the stagnation point, which moves downstream due to the Reynolds number rises. In 2008, Kiwan and Zeitoun [7], performed a research on heat transfer in the porous fin and reported 75% enhancement in heat transfer by the use of porous fins in two concentric cylinders. In addition, they declared the decreasing trend of heat transfer by increasing the attachment angle, unlike solid fins. Furthermore, they showed that the presence of fin on the inner cylinder would change the flow regime in the region between two cylinders. Foams have another advantage regarding fluid availability everywhere due to the continuous and attached flow paths which leads to reduce the size and weight of heat exchangers [8]. According to the obtained results by Liu et al. [9], the lower pressure drop in the foam matrix compared to the crystalline matrix in the same Reynolds number can be concluded. Hoseinzadeh et al. [10] numerically and analytically validated heat transfer in a rectangular cross-section porous fins. It was assumed that the fin is one-dimensional and homogenous, the flow is laminar, and the generated heat is a linear function of temperature. Their results agreed well with other numerical methods. Further, they used the same methods to simulate heat transfer of porous fins in an enclosure [11]. Three different analytical methods are applied to obtain the temperature distribution after deriving the heat transfer equation. The effects of various parameters of natural convection, porosity, Rayleigh numbers are examined in their research. Duwairi et al. [12] considered the MHD mixed convection flow about an isothermal cone embedded in a saturated porous medium. Their results showed that the increasing magnetic strength reduced the heat transfer rates, while increasing the cone angle enhanced the heat transfer rates.

Metal foams are made up of thin metal strings that form a continuum area. Due to the complex shape, different geometries and presence of random surfaces in these bodies along with the lack of knowledge about the actual surface, modeling these objects in the software has always been a problematic issue. Al-azmi and Vafai [13] and [14], simulated a model of open cell foam based on repetition of a unit in eight rows and modeled the fluid flow between these rows with different boundary conditions. Their results indicated the effect of the base metal including its density and other properties, such as the size of the cavities and the strings, etc., on reduction of pressure drop and heat resistance. They also showed that the elasticity of the foam is related to the size of the cavities characterized by the inner diameter of the cavity which is in the range of 0.3 to 4 millimeters. Jiang and Lu [15] studied the heat transfer on a series of sintered spheres in a channel, numerically. They observed that heat transfer would increase with decreasing the size of spheres. In another study [16], they examined the effects of boundary conditions on the natural convection of a sintered plate in a channel to evaluate the heat transfer and pressure drop. Shaik Dawood and Mohamed Nazirudeen [17] developed the technology for making porous gray iron metal foams castings. Box-Behnken Design was applied and density, percentage porosity was

found out. Also, radiography, microstructure, SEM analysis, compression and hardness tests were done.

It was found that in a sintered porous medium, the sintered layer amplifies heat transfer due to the change in the conduction coefficient. In 2002, Cao et al. [18] performed an experimental investigation on the evaporative heat transfer of a sintered copper layer by considering two different sizes of the particles and found optimal porosity for the maximum heat transfer. They also showed that the highest heat transfer rate occurs in the highest porosity percentage. In 2007, Kang et al. [19] experimentally studied the effect of nanofluids with different volume fractions on thermal efficiency of a tube with porous sintered layer. They used silver nanoparticles with diameter of 10 and 35 nanometers and reported the enhancement in thermal performance of the porous heat pipe. Mesgarpour et al. [20-23] examined the effect of contact type, fin shape, sphere diameter, boundary conditions, and variation of Reynolds number on fluid flow and heat transfer in the forced convection around an engineered porous fin with spherical connections in a channel. They showed that using the porous fins with diagonal connections, besides increasing pressure drop, improves thermal performance and increases heat transfer rates compared to parallel connections. They also conducted the use of aluminium and copper with constant heat flux and constant temperature as the boundary conditions in the base of the fin, respectively. Furthermore, they investigated the forced convection flow around a bundle of tapered porous fin in a channel and declared that in lower Reynolds numbers, the use of porous fin is preferred. While in higher Reynolds, solid fins have higher heat transfer and lower pressure drop. They investigated natural convection around the porous fins at different angle of positioning and showed that the best Nusselt number and efficiency will be achieved at 45-degree angle of positioning.

As described in this section, the porous medium offered an effective solution in order to increase heat transfer performance. However, the mechanical strength of the porous fin is another important factor that should be considered carefully for the use of porous medium. According to the literature review, few researches have been conducted about the strength of the porous materials. In 2011, Bouzid et al [24] examined the strength of a porous medium during the drying process and showed that the strength of the porous material in the porous medium is a function of cavity size, material and drying rate. Ito [25] studied the effect of the pressure gradient on the strength and failure of the porous medium. The results showed a logical relationship between the properties of the porous medium and the strength. In 2015, Maurath et al [26] examined the effect of the connection method, the size of cavities and the physical properties on the strength of the sintered fiberglass medium. They also declared the influence of environmental conditions on the quality of sintering process. Hoseinzadeh and Heyns [27] numerically investigated thermo-structural fatigue and lifetime of a heat exchanger as a feed water heater in power plant. They showed that the highest equivalent thermal stresses under these extreme load conditions occur at the joints of the tubes and tubes sheet.

So far, only the issue of heat transfer has been addressed in the discussion of metal foams. Reducing the porosity to

increase heat transfer also reduces the strength of the metal foam. Therefore, the innovation of the present work is the simultaneous study of these two categories and obtaining porosity that satisfies heat transfer and strength simultaneously. In this research, we aim to improve the heat transfer performance and the mechanical strength simultaneously by variation in porosity in an engineered porous medium which has been described in Ref. [22]. The experimental investigation, numerical validation and mesh analysis of heat transfer have been evaluated in this reference. The present work focused on the mechanical strength of the porous copper fin experimentally and numerically. Then, the results of numerical simulation have been obtained for copper, aluminum and brass porous fins to reach the best porosity. Numerical simulation of free convection heat transfer is carried out using STARCCM+ software and numerical analysis of mechanical strength is performed using ANSYS 18.2.

2. Governing equations

In this research, various relationships have been utilized for heat transfer analysis of experimental and numerical results of engineered porous fins. The dimensionless equations of mass, momentum, and energy for incompressible flow by neglecting pressure gradients are expressed as follows [28]:

$$\frac{\partial U_i^*}{\partial x_i^*} = 0, \quad (1)$$

$$\frac{\partial U_i^*}{\partial t^*} + U_i^* \frac{\partial U_i^*}{\partial x_i^*} = \frac{Gr}{Re} \theta + \frac{1}{Re} \frac{\partial^2 U_i^*}{\partial x_j^* \partial x_j^*}$$

$$\frac{\partial \theta}{\partial t^*} + U_i^* \frac{\partial \theta}{\partial x_i^*} = \frac{1}{Re \times Pr} \frac{\partial^2 \theta}{\partial x_i^* \partial x_i^*} + \frac{Ec}{Re} \phi^*$$

In the above equations, U_i^* and θ are the dimensionless velocity components and temperature and respectively. Accordingly, the quantities of the dimensionless parameters are:

$$x^* = \frac{x}{L}, t^* = \frac{t U_\infty}{L}, U^* = \frac{U}{U_\infty}, \theta = \frac{T - T_\infty}{T_b - T_\infty}, \phi^* = \tau_{ij}^* \frac{\partial U_i^*}{\partial x_j^*}, \tau_{ij}^* = \frac{\tau_{ij}}{\frac{1}{2} \rho U_\infty^2} \quad (2)$$

$$Re = \frac{U_\infty L}{\nu}, Pr = \frac{\nu}{\alpha}, Gr = \frac{g \beta (T_s - T_\infty) L_c^3}{\nu^2}, Ec = \frac{U_\infty^2}{C_p (T_s - T_\infty)}$$

In the above equations Re , Gr and Ec are Reynolds, Grashof and Eckert numbers respectively. Since low temperatures are analyzed in this paper, the radiation heat transfer mechanism can be ignored in the fin analysis [29]. Therefore, according to the energy balance in a control volume of fin, neglecting radiation heat transfer, we have:

$$\dot{Q}_{total} = \dot{Q}_{cond} + \dot{Q}_{conv} \quad (3)$$

In the above expression, \dot{Q}_{cond} is the heat transferred through conduction and \dot{Q}_{conv} is the heat transferred through convection. For the conductive and convective heat transfer, we also have:

$$\dot{Q}_{cond} = K_{fin} A_c \frac{\partial T}{\partial x} \quad (4)$$

$$\dot{Q}_{conv} = h A_s (T_s - T_\infty)$$

In the above relations, h is the free convective heat transfer coefficient of the flow, T_s and T_∞ are the of surface and far stream flow temperatures respectively. A_c and A_s are the area of solid cross section and solid surrounding surface respectively and K_{fin} is the thermal conductivity coefficient of the fin. One of the main goals of each experiment and numerical analysis on the convective heat transfer is to find the convective heat transfer coefficients. For this purpose, the average value of this coefficient can be calculated by the following equation:

$$h = \left(\frac{Q_{ave}}{A_s (T_{s,ave} - T_\infty)} \right) \quad (5)$$

In order to model the turbulence in the numerical solution of the heat transfer equations and fluid mechanics, the $k-\varepsilon$ turbulence model is used in this study. The equations of kinetic energy (k) and dissipations (ε) are considered as follows [30]:

$$\frac{\partial}{\partial x_i} (\rho k u_i) + \frac{\partial}{\partial t} (\rho k) \quad (12)$$

$$= \frac{\partial}{\partial x_j} \left(\left(\mu + \frac{\mu_t}{\sigma_k} \right) \frac{\partial k}{\partial x_j} \right) + G_K + G_b - \rho \varepsilon - Y_M + S_K$$

$$\frac{\partial}{\partial x_i} (\rho \varepsilon u_i) + \frac{\partial}{\partial t} (\rho \varepsilon) \quad (13)$$

$$= \frac{\partial}{\partial x_j} \left(\left(\mu + \frac{\mu_t}{\sigma_\varepsilon} \right) \frac{\partial \varepsilon}{\partial x_j} \right) + C_{1\varepsilon} \frac{\varepsilon}{K} (G_K + C_{3\varepsilon} G_b) + C_{2\varepsilon} \rho \frac{\varepsilon^2}{K} + S_\varepsilon$$

In the above-mentioned relationships, G_K represents the production of turbulence kinetic energy in terms of velocity gradient, G_b is turbulence kinetic energy production due to buoyancy forces and Y_M represents the oscillation share in the turbulence density to the total loss; this term is also

known as the turbulence density. $C_{1\varepsilon}$, $C_{2\varepsilon}$ and $C_{3\varepsilon}$ are the constant coefficients and σ_ε and σ_k are the Prandtl coefficients for turbulence. S_K and S_ε are also source terms [30].

For the above equations, it is assumed that flow is three dimensional, incompressible, fully turbulent, and steady. According to the physical nature of the problem, the boundary conditions for different parts of the problem can be defined. These conditions are automatically detected and applied by the STARCCM+ software during solution.

1. Constant temperature and constant heat flux as boundary condition of the fin base.
2. Conduction heat transfer in the Fin
3. The conduction/convection boundary condition on the Fin surface
4. The convection boundary condition in the air around the body

3. Experiments explanation

3.1 Test sample

In order to study the effect of porosity on heat transfer and fin performance, as well as evaluating fin strength, an engineered copper porous fin is manufactured by casting method as shown in Figure 1. As can be concluded from Table 1, by comparing engineered porous fin with spherical connections and a rigid fin with identical dimensions, 42% reduction in fin volume and mass would be achieved. This reduction is accompanied with 21.72% increase in surface area. Therefore, besides the improving of heat transfer performance, the amount of material needed to produce the fin has decreased.

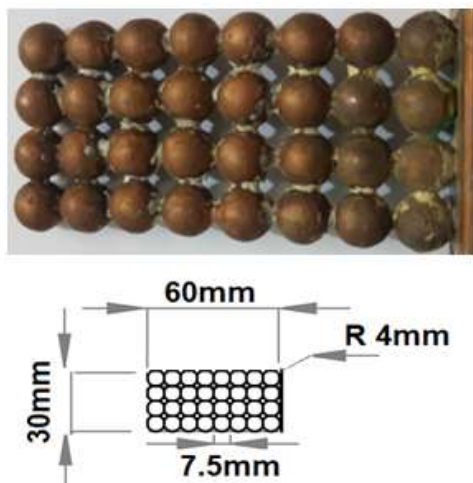


Figure 1: Manufactured engineered porous fin and its dimensions

3-2 Tensile strength test

To evaluate the tensile strength of a porous fin, as described in Section 3.1, tensile test has been carried out at the Razi Reference Laboratory in Tehran, with reference standards. The results have been extracted in the form of strain-stress diagrams. The apparatus used for tensile test is INSTRON 8502 model with the power of 25 tons, which is composed of two jaws; an upper moving jaw and a lower fixed jaw. The stress is applied to the sample by the moving jaw with a frequency of 100 times per second, so the sample has been stretched up to its fracture point. Then the engineering stress-strain curve has been obtained by recording the applied force and the corresponding strain. The system can also provide complete information, such as yield stress and strain, necking, fracture, plastic strain of fracture, energy up to the yield and fracture strengths, as well as Young's modulus. The specification of the tensile testing apparatus is presented in Table 2. This apparatus includes the following sub-sections: force gauge, micrometers and laser distance meter. The accuracy and uncertainty of equipment are provided in Table 3.

Table 2: Specification of the tensile testing apparatus

Characteristic	Value
capacity (kgf)	2000
distance between columns (mm)	400
Jaw velocity (mm/min)	500
Maximum distance (mm) between two jaws	700
accuracy of measuring (mm) displacement	0.01
Force measurement resolution	1/20000
Force measurement accuracy	0.5%

Table 3: Accuracy and uncertainty of tensile test measurement devices

device	Accuracy	Uncertainty
Load cell	C4 class	
Micrometer	5 μ m	0.0028
Laser rangefinder	0.02mm	0.011

Table 1: Geometry and mass comparison of rigid and porous fin with identical dimension constructed in the present study

parameter	rigid fin	porous fin	percent of variation in porous fin relative to rigid one (%)
volume (mm^3)	21888/00	12729/54	-41/84
surrounding surface (mm^2)	7232/00	8803/43	21/72
mass (gr)	194/8	113/29	-41/84

3-2 Tensile strength test

To evaluate the tensile strength of a porous fin, as described in Section 3.1, tensile test has been carried out at the Razi Reference Laboratory in Tehran, with reference standards. The results have been extracted in the form of strain-stress diagrams. The apparatus used for tensile test is INSTRON 8502 model with the power of 25 tons, which is composed of two jaws; an upper moving jaw and a lower fixed jaw. The stress is applied to the sample by the moving jaw with a frequency of 100 times per second, so the sample has been stretched up to its fracture point. Then the engineering stress-strain curve has been obtained by recording the applied force and the corresponding strain. The system can also provide complete information, such as yield stress and strain, necking, fracture, plastic strain of fracture, energy up to the yield and fracture strengths, as well as Young's modulus. The specification of the tensile testing apparatus is presented in Table 2. This apparatus includes the following sub-sections: force gauge, micrometers and laser distance meter. The accuracy and uncertainty of equipment are provided in Table 3.

Table 2: Specification of the tensile testing apparatus

Characteristic	Value
capacity (kgf)	2000
distance between columns (mm)	400
Jaw velocity (mm/min)	500
Maximum distance between two (mm) jaws	700
accuracy of measuring (mm) displacement	0.01
Force measurement resolution	1/20000
Force measurement accuracy	0.5%

Table 3: Accuracy and uncertainty of tensile test measurement devices

device	Accuracy	Uncertainty
Load cell	C4 class	
Micrometer	5 μ m	0.0028
Laser rangefinder	0.02mm	0.011

4. Numerical modeling method

4-1- Modeling of heat transfer

All Numerical modeling methods for heat transfer simulation, such as software, solution method, assumptions,

viscosity model, boundary conditions, convergence criterion and discretization method have been described in ref. [22].

4-2- Modeling the strength

The tensile strength has been evaluated numerically with ANSYS workbench software. In static structure mode, after meshing, the model of the fin is subjected to fixed base and axial force boundary conditions. Generally, in solid analysis techniques and finite element methods, analysis of the grid is not of great importance. However, in this research, the accuracy of the grid is also investigated. In order to determine yield and fracture limit of the piece, yield strength is considered as a criterion according to the material properties references and imported to the software. In numerical analysis, it is possible to study the fatigue phenomenon based on the working cycle. As no results are available for fatigue validation, only a tensile stress analysis is performed. The calculation time of the numerical analysis is about 124 minutes.

5. Results and discussion

The validity of the numerical results for heat transfer analysis have been performed in previous work [22]. For experimental validation, the comparison of temperature distribution with analytical results reveals a maximum error of 1.5%. For Nusselt number 6 percent difference was reported. For validation of numerical results, the maximum error value is about 3.1% in numerical calculations of temperature distribution along the fin length in three different angles. According to this reference, the mesh independency has been checked, and a grid with 455,789 nodes has been selected.

5-1- Investigating the tensile strength test

The main difference between porous and rigid fins subjected to tensile forces and corresponding stresses is the cross-section area. In other words, the cross-section area of the porous fins varies as a periodic function, while it is constant for the rigid fin. The results of stress and strain for porous copper fins extracted from the tensile test apparatus and the final fractured fin are depicted in Figure 2. According to this diagram, although the copper fin requires higher force for deformation, the deformation in fracture zone is low, while it has a wide area of plastics deformation.

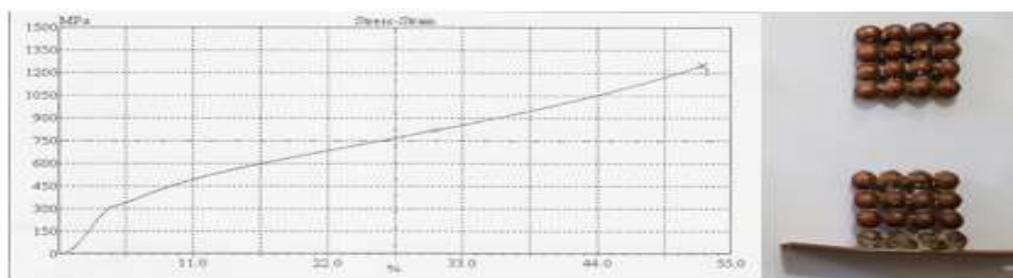


Figure 2: Stress-strain diagram for porous copper fin and its final fracture

5-2- Numerical Analysis:

Figure 3 shows the mesh independency and generated grid on the porous copper fin. The uniform and coherent grid is of great importance in stress-strain analysis. The mesh number is selected 4000 due to mesh independency and it is unstructured.

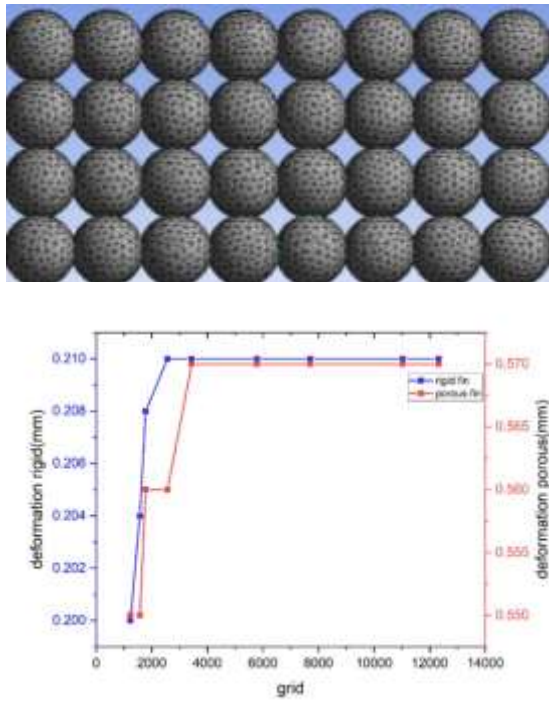


Figure 3: Mesh independency and generated grid on a porous copper fin

Figure 4 shows the deformation versus the applied force for numerical and experimental results. As can be seen, the numerical results provide an accurate estimation of the stress-strain relationship for a porous fin sample especially for higher forces.

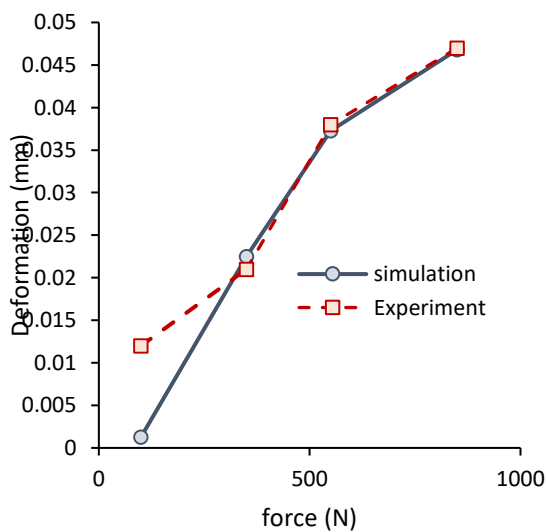


Figure 4: Comparing deformation versus applied force for numerical and experimental results

To compare the tensile strength of the porous and rigid fins with the same dimensions, it can be referred to the numerical results of Figure 5. As expected, the deformation

according to the maximum force is almost twice for the porous fin relative to rigid one. The deformation of the rigid fin at the maximum force of 10,000 N is 0.04 millimeters, while this value is equal to 0.777 millimeter for the porous fin. So, it can be concluded that the deformation of the porous fin is higher, and consequently, the strength of the porous fin is lower compared to the rigid one. The reason for this is due to the reduction of the fin cross section at the points where the spheres connect to each other. By reducing the cross section for a constant force, the applied stress and the consequently resulting strain increase. Furthermore, the location of the lowest thickness is the most suitable candidate for fracture (see figure 2).

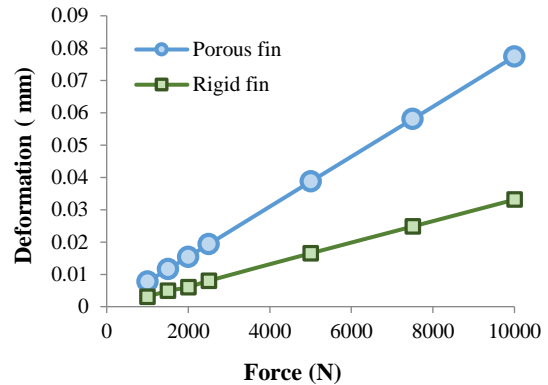


Figure 5: Deformation versus Force for the porous and rigid fins with the same dimensions

5-3- Estimation of the best porosity

The results of the strength analysis indicate less strength of the porous fin due to the presence of areas with low thickness. On the other hand, the results of heat transfer analysis, showed the superior performance of the porous fin. The most important issue is the selection of the middle condition for the fin porosity, in which the best possible strength and thermal performance are achieved simultaneously.

According to Figure 6, four fin models are plotted by considering the distance of the spheres' centers as a variable. The minimum and the maximum possible distances are selected considering the rigidity and integrity of the fin respectively. It can be seen that with increasing the distance of the spheres' center, the porosity percentage changes according to Table 4. This change in the porosity is associated with increasing the length and the width of the piece.

Table 4: Geometric specifications of porous fins with different porosity

distance between two balls	Surrounding surface area (mm ²)	Volume (mm ³)	Porosity percentage
6	5600.62	10821.44	27.11853
6.5	6653.56	11633.72	31.56635
7	7705.16	12234.09	36.59779
7.5	8754.97	12606.28	42.00276

The obtained results show that increasing the distance between two balls leads to enhancement in the porosity percentage, which would intensify the share of thermal convection in heat transfer consequently. On the other hand, increasing the porosity leads to a decrease in strength as can be concluded from Table 5. As well, the behavior of the thermal convective heat transfer coefficient for different porosity under the constant temperature and the constant thermal flux boundary conditions in the fin base is distinct.

Table 5: Tensile strength and heat transfer coefficient for different porosity percentage

Porosity percentage	Max. Tensile strength	Convective Heat transfer coefficient for constant heat flux in the base (W/m^2K)	Convective Heat transfer coefficient for constant temperature in the base (W/m^2K)
27.1	120.3369	7.163	33.464
31.6	102.459	8.633	33.765
36.6	82.23684	8.125	85.736
42	55.4939	7.578	47.321

In Figure 7, the variation of the convective coefficient and strength versus the porosity percentage is shown for the constant flux and the constant temperature boundary conditions at the base for three materials (copper, aluminum and brass). According to this diagram, it is clear that in all of these states, the heat transfer coefficient at a specific porosity is the maximum (36.6% for brass and aluminum fins and 31.6% for copper fin) and it is reduced with further increase in the porosity. The reason is due to reduction in cross section area of heat transfer and consequently decrease in the conductive heat transfer between the spheres. In this porosity, in fact, the sum of the conduction heat transfer between the spheres and the convective heat transfer from the spheres to the fluid reaches its highest value. As the percentage of porosity increases, decrease in conduction heat transfer is more sharply than increase in convective heat transfer. The highest tensile strength is achieved for the aluminum fin and the strength of the copper

and the brass fins are similar. This fact is related to the modulus of elasticity of these materials and because copper and brass have a higher modulus of elasticity than aluminum, they have less elastic deformation and fail sooner. By increasing the porosity the strength of the fin decreases for all materials because of reduction in cross section area in connection points.

The best conditions obtained with regard to the cross-point of two curves in this graph. This porosity for the porous fins of different material with different boundary conditions of the fin base are presented in Table 6.

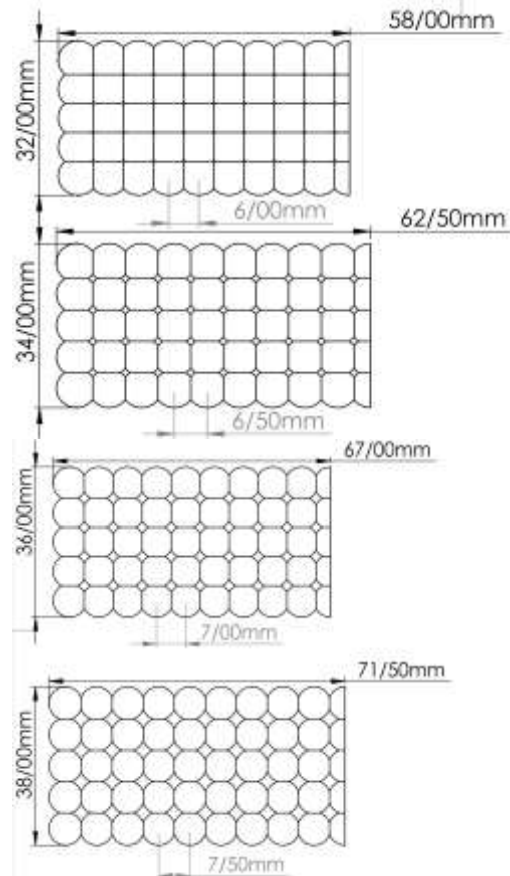


Figure 6: Geometric dimensions of porous fins with different porosity

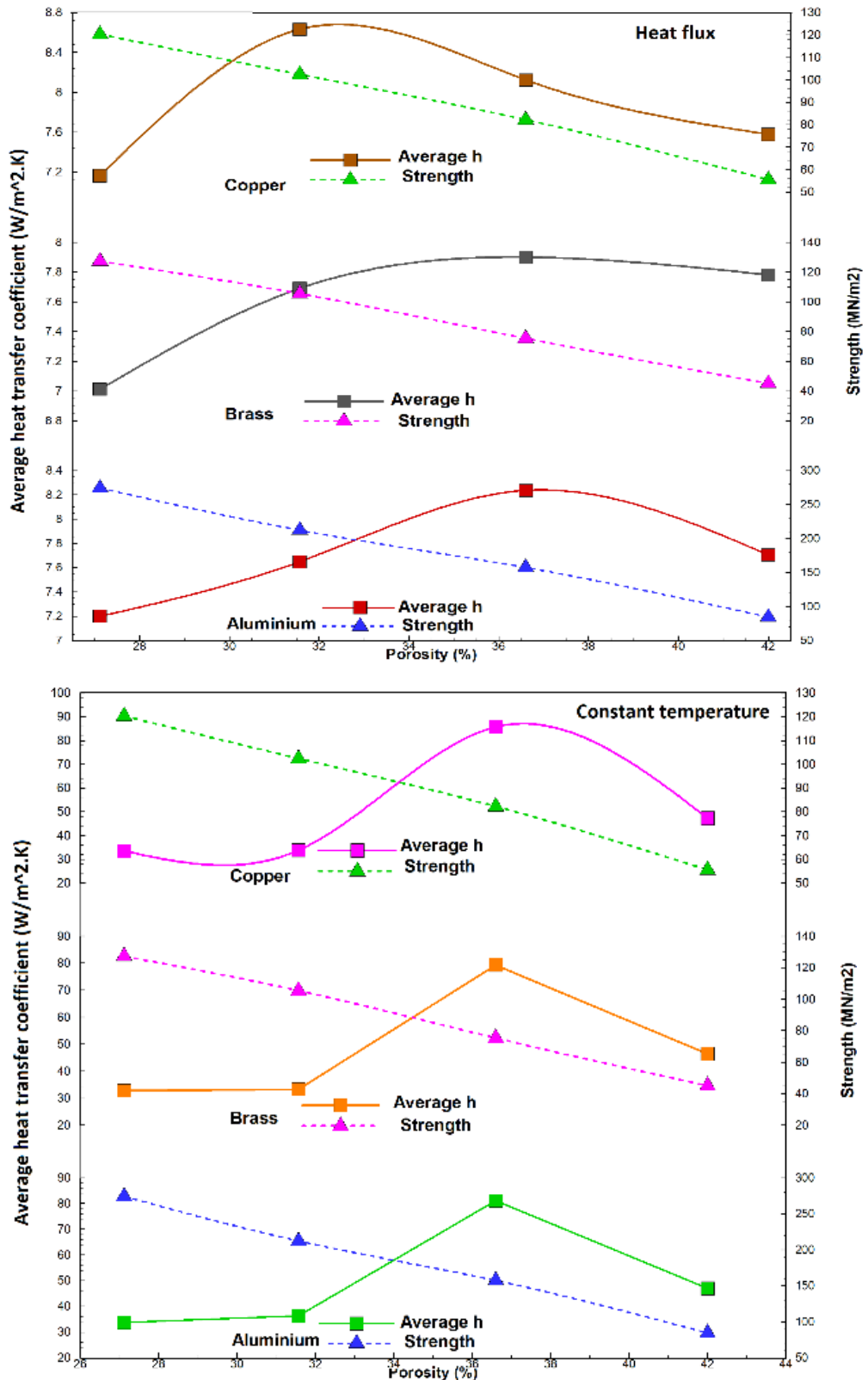


Figure 7: Variation of the convective heat transfer coefficient and strength versus the porosity percentage with different materials for (a) constant flux and (b) constant temperature boundary conditions at the base

Finding the optimum porosity for satisfying the best possible heat transfer and strength simultaneously is the most important innovation of this research. The main restriction for using these results is that:

- The Rayleigh number should be within the laminar free convection range.
- The manufacturing conditions have no effect on strength.
- The porosity percentage is constant in all directions.

Table 6: the optimal porosity for satisfying the best possible heat transfer and strength simultaneously for different materials and different boundary conditions at the base

material	constant flux at the base	constant temperature at the base
Copper	30.1%	34.2%
Aluminum	31.4%	34.5%
Brass	32.7%	34%

6. Conclusion

In this research, with experimental and numerical analysis of free convection heat transfer and strength in engineered porous fin, the best porosity satisfies the heat transfer and the strength simultaneously in different boundary conditions of the base and three different materials of the fin. The following consequences have been conducted:

- The results show that the strength decreases with increasing the porosity percentage.
- It has been found that for a specific porosity, the strength and the heat transfer are simultaneously satisfactory. This value of porosity varies from one material to another and it depends on the boundary condition of the base.
- If the boundary condition of the base is selected as a constant temperature, the best porosity is obtained around 34% for all materials which is higher than the best porosity for constant heat flux boundary condition (around 31%).
- For maximum heat transfer point of view for constant heat flux at the base, the best porosity among the studied porosity percentage is 36.6% for brass and aluminum fins and 31.6% for copper fin. However, it is calculated 36.6% for all materials for constant temperature at the base.

References

- [1] I. J. J. Zahmatkesh, "Heatline visualization of buoyancy-driven flow inside a nanofluid-saturated porous enclosure," vol. 9, no. 2, 2015.
- [2] I. Zahmatkesh, S. A. J. J. J. o. M. Naghedifar, and I. Engineering, "Pulsating Nanofluid Jet Impingement onto a Partially Heated Surface Immersed in a Porous Layer," vol. 12, no. 2, 2018.
- [3] Z. Uddin, M. J. J. J. o. M. Kumar, and I. Engineering, "MHD Heat and Mass Transfer Free Convection Flow near The Lower Stagnation Point of an Isothermal Cylinder Imbedded in Porous Domain with the Presence of Radiation," vol. 5, no. 2, 2011.
- [4] M. Hatami and D. Ganji, "Thermal performance of circular convective-radiative porous fins with different section shapes and materials," *Energy Conversion and Management*, vol. 76, pp. 185-193, 2013.
- [5] A. M. Morega, A. J. I. J. o. H. Bejan, and M. Transfer, "Heatline visualization of forced convection laminar boundary layers," vol. 36, no. 16, pp. 3957-3966, 1993.
- [6] T.-M. Jeng, S.-C. J. I. J. o. H. Tzeng, and M. Transfer, "Numerical study of confined slot jet impinging on porous metallic foam heat sink," vol. 48, no. 23-24, pp. 4685-4694, 2005.
- [7] S. Kiwan and O. Zeitoun, "Natural convection in a horizontal cylindrical annulus using porous fins," *International Journal of Numerical Methods for Heat & Fluid Flow*, vol. 18, no. 5, pp. 618-634, 2008.
- [8] S. Mahjoob and K. Vafai, "A synthesis of fluid and thermal transport models for metal foam heat exchangers," *International Journal of Heat and Mass Transfer*, vol. 51, no. 15, pp. 3701-3711, 2008.
- [9] J. Liu, W. Wu, W. Chiu, and W. Hsieh, "Measurement and correlation of friction characteristic of flow through foam matrixes," *Experimental thermal and fluid science*, vol. 30, no. 4, pp. 329-336, 2006.
- [10] S. Hoseinzadeh, A. Moafi, A. Shirkhani, A. J. J. J. o. T. Chamkha, and H. Transfer, "Numerical validation heat transfer of rectangular cross-section porous fins," vol. 33, no. 3, pp. 698-704, 2019.
- [11] S. Hoseinzadeh, P. S. Heyns, A. J. Chamkha, and A. Shirkhani, "Thermal analysis of porous fins enclosure with the comparison of analytical and numerical methods," *Journal of Thermal Analysis and Calorimetry*, vol. 138, no. 1, pp. 727-735, 2019/10/01 2019.
- [12] H. Duwairi, O. Abu-Zeid, A. D. J. J. J. o. M. Rebhi, and I. Engineering, "Viscous and Joule heating effects over an isothermal cone in saturated porous media," vol. 1, no. 2, pp. 113-118, 2007.
- [13] K. Vafai, "Analysis of variable porosity, thermal dispersion, and local thermal nonequilibrium on free surface flows through porous media," 2004.
- [14] B. S. Al-azmi and K. Vafai, "Analysis of variants within the porous media transport models," Ohio State University, 2000.
- [15] P.-X. Jiang, X.-C. J. I. J. o. H. Lu, and M. Transfer, "Numerical simulation of fluid flow and convection heat transfer in sintered porous plate channels," vol. 49, no. 9-10, pp. 1685-1695, 2006.
- [16] P.-X. Jiang, M. Li, Y.-C. Ma, Z.-P. J. I. J. o. H. Ren, and M. Transfer, "Boundary conditions and wall effect for forced convection heat transfer in sintered porous plate channels," vol. 47, no. 10-11, pp. 2073-2083, 2004.
- [17] S. J. M. I. E. Nazirudeen, "A Development of Technology for Making Porous Metal Foams Castings," *Jordan Journal of Mechanical and Industrial Engineering*, vol. 4, pp. 292-299, 2010.
- [18] X. Cao, P. Cheng, T. J. J. o. t. Zhao, and h. transfer, "Experimental study of evaporative heat transfer in sintered copper bidispersed wick structures," vol. 16, no. 4, pp. 547-552, 2002.
- [19] S.-W. Kang, W.-C. Wei, S.-H. Tsai, and C.-C. J. A. T. E. Huang, "Experimental investigation of nanofluids on sintered heat pipe thermal performance," vol. 29, no. 5-6, pp. 973-979, 2009.
- [20] M. Mesgarpour, A. Heydari, and S. Soddodin, "Investigating the effect of connection type of a sintered porous fin through a channel on heat transfer and fluid flow," *Journal of Thermal Analysis and Calorimetry*, pp. 1-14.
- [21] M. Mesgarpour, A. Heydari, and S. Saedodin, "Numerical analysis of heat transfer and fluid flow in the bundle of porous tapered fins," *International Journal of Thermal Sciences*, vol. 135, pp. 398-409, 2019.
- [22] M. Mesgarpour, A. Heydari, and S. Saedodin, "Comparison of free convection flow around an engineered porous fin with spherical connections and rigid fin under different positioning angles—An experimental and numerical analysis," *Physics of Fluids*, vol. 31, no. 3, p. 037110, 2019.
- [23] M. Mesgarpour and A. Heydari, "Numerical investigation of heat transfer in a sintered porous fin in a channel flow with the aim of material determination," *Journal of Heat and Mass Transfer Research*, vol. 6, no. 1, pp. 63-74, 2019.
- [24] M. Bouzid, L. Mercury, A. Lassin, J. M. Matray, and M. Azaroual, "In-pore tensile stress by drying-induced capillary bridges inside porous materials," *J Colloid Interface Sci*, vol. 355, no. 2, pp. 494-502, Mar 15 2011.

- [25] T. J. E. F. M. Ito, "Effect of pore pressure gradient on fracture initiation in fluid saturated porous media: Rock," vol. 75, no. 7, pp. 1753-1762, 2008.
- [26] J. Maurath, J. Dittmann, N. Schultz, N. J. S. Willenbacher, and P. Technology, "Fabrication of highly porous glass filters using capillary suspension processing," vol. 149, pp. 470-478, 2015.
- [27] S. Hoseinzadeh and P. S. Heyns, "Thermo-structural fatigue and lifetime analysis of a heat exchanger as a feedwater heater in power plant," *Engineering Failure Analysis*, vol. 113, p. 104548, 2020/07/01/ 2020.
- [28] L. Leal, *Advanced Transport Phenomena: Fluid Mechanics and Convective Transport Processes*. Cambridge University Press, 2007.
- [29] R. S. R. Gorla and A. Y. Bakier, "Thermal analysis of natural convection and radiation in porous fins," *International Communications in Heat and Mass Transfer*, vol. 38, no. 5, pp. 638-645, 2011/05/01/ 2011.
- [30] H. K. Versteeg and W. Malalasekera, *An introduction to computational fluid dynamics: the finite volume method*. Pearson education, 2007.